



Cite this: *RSC Adv.*, 2021, **11**, 22327

Mechanically and electrically durable, stretchable electronic textiles for robust wearable electronics[†]

Sun Hong Kim, [‡]^a Yewon Kim, [‡]^b Heewon Choi, ^b Juhhyung Park, ^a Jeong Han Song, ^a Hyoung Won Baac, ^b Mikyung Shin, ^{ef} Jeonghun Kwak ^{*a} and Donghee Son^{*bcd}

A monolithic integration of high-performance soft electronic modules into various fabric materials has enabled a paradigm shift in wearable textile electronics. However, the current textile electronics have struggled against fatigue under repetitive deformation due to the absence of materials and structural design strategies for imparting electrical and mechanical robustness to individual fibers. Here, we report a mechanically and electrically durable, stretchable electronic textile (MED-ET) enabled by a precisely controlled diffusion of tough self-healing stretchable inks into fibers and an adoption of the kirigami-inspired design. Remarkably, the conductive percolative pathways in the fabric of MED-ET even under a harshly deformed environment were stably maintained due to an electrical recovery phenomenon which originates from the spontaneous rearrangement of Ag flakes in the self-healing polymer matrix. Specifically, such a unique property enabled damage-resistant performance when repetitive deformation and scratch were applied. In addition, the kirigami-inspired design was capable of efficiently dissipating the accumulated stress in the conductive fabric during stretching, thereby providing high stretchability (a tensile strain of 300%) without any mechanical fracture or electrical malfunction. Finally, we successfully demonstrate various electronic textile applications such as stretchable micro-light-emitting diodes (Micro-LED), electromyogram (EMG) monitoring and all-fabric thermoelectric devices (F-TEG).

Received 30th April 2021
 Accepted 16th June 2021

DOI: 10.1039/d1ra03392a
rsc.li/rsc-advances

1 Introduction

Textile electronics is an emerging field involving technology that enables the incorporation of a variety of wearable applications, such as deformable sensor networks, displays,¹⁻³ circuits,⁴ and energy-harvesting devices, on clothing.⁵⁻⁷ For an integrated system on clothing, a stretchable conductor is essential for connecting the devices and ensuring high performance. Recently, there has been some progress in textile electronics using weaving⁸⁻¹⁰ and knitting¹¹⁻¹³ processes with functional fibers that require additional techniques and

equipment. Furthermore, electronic textiles can also be fabricated *via* the coating of single-walled carbon nanotubes,^{14,15} conductive polymers,¹⁶⁻¹⁸ silver nanowires,^{19,20} and metal plating.²¹ However, this approach suffers from limitations in terms of mechanical durability owing to the weak interaction between the nanomaterials and textiles. By contrast, composite inks²²⁻²⁸ are promising candidates for fabricating stretchable textile electronics, as they require simple and low-cost processes. Although the surfaces of textiles have complex geometry, mechanical robustness can be realized *via* the penetration of these composite inks into textiles. In addition, various functions could be imparted on the fabric by changing the filler materials. With these materials, many kinds of stretchable textiles have been developed for demonstrating smart textile electronics, but currently available stretchable textile materials are still associated with certain challenges, such as the modulus mismatch at the skin, and limited stretchability. To overcome these issues, a kirigami-inspired pattern has been applied to textiles. Kirigami, which refers to the cutting of materials into certain patterns to achieve stress dissipation, has excellent potential for realizing the desired stretchable electronic properties. In conventional kirigami-inspired electronics, cut patterns were introduced into a sheet of paper or films to attain a desirable topology on folding.²⁹⁻³² Furthermore, this technique has been extended for engineering materials in a small scale for imparting high stretchability to intrinsically rigid

^aDepartment of Electrical and Computer Engineering, Inter-University Semiconductor Research Center, Seoul National University, Seoul, 08826, Republic of Korea. E-mail: jkwak@snu.ac.kr

^bDepartment of Electrical and Computer Engineering, Sungkyunkwan University, Suwon, 16419, Republic of Korea. E-mail: daniel3600@g.sku.edu

^cCenter for Neuroscience Imaging Research, Institute for Basic Science (IBS), Sungkyunkwan University (SKKU), Suwon, 16419, Republic of Korea

^dDepartment of Superintelligence Engineering, Sungkyunkwan University (SKKU), Suwon, 16419, Republic of Korea

^eDepartment of Biomedical Engineering, Sungkyunkwan University (SKKU), Seobu-ro 2066, Jangan-gu, Suwon, 16419, Gyeonggi-do, Korea

^fDepartment of Intelligent Precision Healthcare Convergence, Sungkyunkwan University (SKKU), Seobu-ro 2066, Jangan-gu, Suwon, 16419, Gyeonggi-do, Korea

† Electronic supplementary information (ESI) available. See DOI: [10.1039/d1ra03392a](https://doi.org/10.1039/d1ra03392a)

‡ These authors contributed equally: Sun Hong Kim, Yewon Kim.



materials.^{33–36} Recently, an unconventional strategy to create robust, kirigami-inspired e-textiles with enhanced electromechanical features was demonstrated.³⁷ However, the durability of electronic textiles under harshly damaged conditions have not been reported yet.

Herein, we report a kirigami-patterned stretchable electronic textile showing electrical recoverability under harshly damaged conditions and high stretchability with a minimal change in resistance. The MED-ET was fabricated *via* a soaking process (Fig. 1a) that enables highly conductive and stretchable wiring on textiles in a simple and inexpensive manner. The tough self-healing stretchable ink used consists of a dynamically cross-linked self-healing polymer [poly(dimethylsiloxane), 4,4-methylenebis(phenyl urea), and isophorone bisurea (PDMS-MPU_{0.4}-IU_{0.6})], Ag flakes and organic solvent.^{38,39} This tough self-healing stretchable composite penetrated well into the polyurethane-based fabric, providing mechanical robustness (Fig. 1b). A cross-sectional scanning electron microscopy (SEM, JSM-7600F Schottky field emission scanning electron microscope, JEOL USA, Inc, Japan) image of the conductive fabric shows that the conductive composite was well penetrated between the fiber bundles as shown in Fig. 1c. We adopted the kirigami-inspired pattern to impart the conventional stretchable polyurethane-based fabric with a high stretchability of over 300%. In addition, it shows minor change in resistance ($\Delta R/R_0 \sim 0.35$) at a strain of 300%. To improve its mechanical and electrical stability, we applied heat and pressure to the MED-ET.⁴⁰ Lastly, we employed the MED-ET in various applications, including

a stretchable micro-light-emitting diode (Micro-LED), an electromyogram (EMG) sensor, and a thermoelectric generator.

2 Experimental details

2.1 Fabrication process for the MED-ET

Prior to fabricating the MED-ET, we investigated the uniformity in the areal electrical performance. This was measured by testing nine regions ($10 \text{ mm} \times 10 \text{ mm}$ circles) over an area of 49 cm^2 ($7 \text{ cm} \times 7 \text{ cm}$ square) (Fig. 2a). The line resistance was determined to be $1.8\text{--}3.2 \Omega$. Hence, it was concluded that the soaked fabric is uniformly conductive. The proposed MED-ET was fabricated using a simple process (Fig. 2b and S1). First, we prepared the tough self-healing stretchable ink, which was used to impart conductivity to the fabric. For preparing tough self-healing stretchable ink, we added 1 g of a self-healing polymer (SHP, PDMS-4,4-methylenebis(phenyl urea) (MPU)_{0.4}-isophorone bisurea units (IU)_{0.6}) in 8 mL of 4-methyl-2-pentanone (MIBK, Sigma Aldrich 360511), and the mixture was stirred for 1 h. After the SHP was completely dissolved, we added 4 g of Ag flakes (Daejoo Electronics, DSF-500 MWZ-S) to the SHP solution and stirred it for 1 h to ensure complete dispersion. Next, we cut the polyurethane fabric into a rectangular shape ($4 \text{ cm} \times 2 \text{ cm}$) and soaked it in the prepared ink for several seconds. Soaking the fabric into the tough self-healing stretchable ink prepared in a glass dish allowed the ink to permeate into the textile and become immobilized inside of the fiber bundles as the ink dries. Consequently, the self-healing stretchable conductor formed intrinsically stretchable conductive paths inside of the fiber bundles. Interestingly, after the drying process, the Ag composite rich region was observed on the surface of the conductive fabric. Before the solidification process is completed, the soaked ink sank to the bottom by gravity from the fabric. Actually, the Ag composite rich region of conductive fabric showed lower resistance value than that of opposite surface (Fig. S2†). Thanks to this Ag composite rich region on the surfaces, we have two advantages: (i) reducing contact resistance between our conductive fabric and external

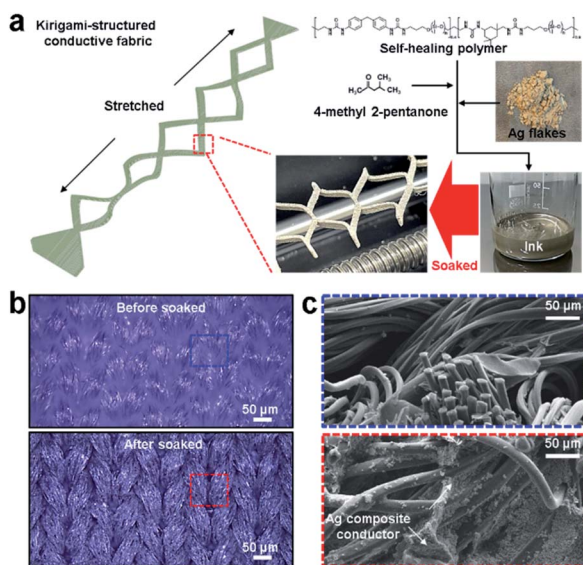


Fig. 1 Highly stretchable, MED-ET fabricated by soaking process of tough self-healing stretchable Ag ink. (a) Schematic showing the highly stretchable, MED-ET fabricated *via* a simple soaking process. The conductive ink consists of a self-healing polymer, organic solvents (MIBK), and Ag flakes. (b) Optical microscopy image of the fabric before (top) and after (bottom) the soaking process. The scale bar is $50 \mu\text{m}$ (c) cross-sectional SEM image of the textile before and after the soaking process; the scale bars are $50 \mu\text{m}$.

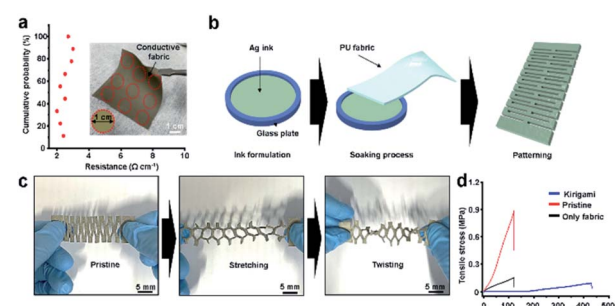


Fig. 2 Fabrication process and strain–stress characterization of MED-ET. (a) Cumulative probability indicating the uniformity in the electrical performance of the rectangular conductive fabric. (b) Fabrication process for MED-ET. (c) Sequential process of deformation: pristine, stretching, and twisting (d) strain–stress curves of three fabrics: polyurethane fabric (only fabric; black), conductive fabric without the kirigami pattern (pristine; red), and kirigami conductive fabric (kirigami; blue).



modules and (ii) providing robust layer on the surface of fabric for electrical and mechanical recoverability. After the conductive fabric was completely dried, we designed a conductive fabric in kirigami shape that could be stretched in one direction *via* uniaxial patterning. We employed a simple centered rectangular arrangement of cuts with dimensions set to the following: length (L), width (W), horizontal cut-spacing (H_c) = 1 mm; vertical cut-spacing (V_c) = 15 mm; center cut length (L_c) = 5 mm and number of cuts (N) = 9 (Fig. S3†). The kirigami shape used can be stretched perpendicular to the cutting direction, and when stretched, a diamond-line pattern with round corners is formed (Fig. 2c). Owing to this design, the modulus of the conductive fabric decreased, and the applied external stress was effectively dissipated (Fig. 2d, S4).

2.2 Measurement setup for the characterization of the MED-ET

To measure the mechanical and electrical characteristics of the MED-ET, we used a digital multimeter (Keithley 2450 source meter, Tektronics) and a motor-based one-axis stretcher (SMC-100, Jaeil optical system) for the stretching and cyclic tests, respectively. We prepared three samples: pristine conductive fabric, MED-ET, and heat- and pressure-treated MED-ET.

To measure the stretchability of samples, we loaded the sample on the stretcher using double-sided tape; the initial length before stretching was set to 2.5 cm. Using this process, we can prevent errors during the measurements, such as the slipping of a loaded sample. Electrical wires were used to connect the digital multimeter to samples. We stripped the end of the sheath and fixed it with 3M tape. Subsequently, we connected the electrical wires with the multimeter. To ensure a stable electrical contact between the wire and the sample, we added several drops of liquid metal (Alfa Aesar, 12478) to the contact area. The stretching speed was 3 mm min⁻¹. The change in resistance with respect to the stretching time was obtained using the software of the digital multimeter and plotted. Also, during the measurement, the completely stretched sample was observed for 1 h to elucidate the electrical recovery related to the dynamic SHP matrix behaviors.³⁸

To measure sample durability, cyclic testing was performed. We loaded the sample on the stretcher and contacted it with a digital multimeter, similar to that in the stretching test. The cyclic tests were performed at a strain of 25% over 100 cycles. For the heat- and pressure-treated samples, 150 °C and 71.3 N m⁻², respectively, were applied for 30 min.

2.3 Fabrication of a micro-LED interconnected with the MED-ET

We prepared a sample for light emission by connecting a micro-LED between two MED-ET samples. To improve the connection between the micro-LEDs and the kirigami-inspired conductive fabric, we soldered both sides of the micro-LEDs and used a silicon adhesive (Silpoxy, Smooth-on Inc.) for physical adhesion and liquid metal for stable electrical contact.

2.4 Measurement setup for real-time EMG monitoring

We used three MED-ET samples, three hook-type electrodes for the connections, and data acquisition equipment (DAQ, PowerLab 8/35) to monitor the electromyogram signals produced during arm muscle movement.^{38,40} To ensure that the samples were attached to the skin thoroughly, 3M Tegaderm films were used.

2.5 Measurement setup for thermoelectric generator

The thermoelectric properties were determined using a home-made stage consisting of two Peltier modules controlled using a Keithley 2200 power supply and a Keithley 2601B source meter. Two individual T-type thermocouples were used to detect the temperatures of the hot and cold sides of the film. The generated thermovoltage was measured using a Keithley 2182A nanovoltmeter. The temperature gradient ranged from -5 to 5 K, and the mean temperature remained fixed at 300 K. The Seebeck coefficients (S) were extracted *via* linear fitting of the thermovoltage-temperature difference data points ($S = \Delta V/\Delta T$).

3 Result and discussion

3.1 Stretchability test of the conductive fabrics

To compare the stretchability of the MED-ET with that of the pristine conductive fabric and heat- and pressure-treated MED-ET, we performed a stretching test using an auto-stretcher. The relative resistance changes ($\Delta R/R_0$) for the three conductive fabrics subjected to stretching are shown in Fig. 3a. The pristine polyurethane-based conductive fabric failed at a strain of 110% and exhibited a 25-fold increase in resistance, relative to the initial value. Thin, composite conductor film coated on a three-dimensional surface are strongly affected by the deformation of a fabric with a relatively large modulus (Fig. S1†). Hence, an

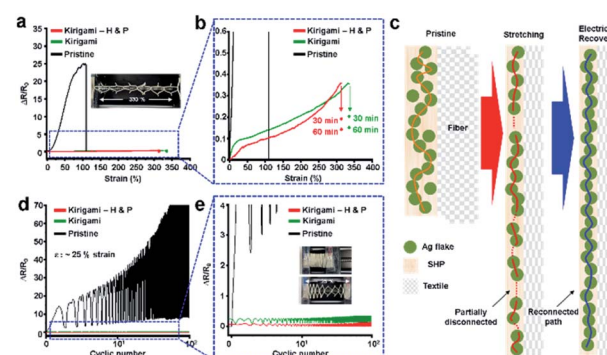


Fig. 3 Mechanical and electrical characterizations of conductive fabrics. (a) Relative change in resistance of the pristine conductive fabric (pristine; black), MED-ET (kirigami; green), and heat- and pressure-treated MED-ET (kirigami-H&P; red) under stretching. (b) Magnified graph of (a) showing the electrical recovery of MED-ET (green) and the heat- and pressure-treated MED-ET (red) at a strain of 330% after 30 min and 1 h, respectively. (c) A schematic illustration showing dynamic behaviors of Ag flakes which make conductive pathways in the SHP matrix when stretched and electrical recovered. (d), (e) Relative changes in the resistance of the three conductive fabrics under a cyclic strain of 25%.



abrupt change in resistance was observed for the pristine conductive fabric. By contrast, the MED-ET exhibited only a 1.5-fold increase in resistance, because the geometry of the kirigami pattern provides high degree of deformability to conductive fabric. Furthermore, heat and pressure were applied to the MED-ET to enhance the mechanical stability between the conductive composite and the polyurethane-based fabric and to decrease the change in the resistance of the conductive fabric when the MED-ET is subjected to strain.⁴⁰

3.2 Electrical recovery of the MED-ET

In many wearable applications, an instantaneous degradation of the device performance could occur, resulting in permanent failure to devices. In terms of long-term usability, mechanical durability is very important. Interestingly, in our MED-ET, electrical recovery through the rearrangement of Ag flakes in the SHP matrix was observed under tensile strain.^{38,41} We investigated the change in the resistance of the conductive fabric in real time as the sample was stretched under a strain of 330% (Fig. 3b). We observed that the resistance decreased with time and that the final relative change in resistance was ~ 0.15 , which is half of its maximum value. Fundamentally, we hypothesized that this phenomenon is probably related to the dynamic behavior of the SHP matrix. Specifically, Ag flakes can be reconnected in the free volume of the relaxed polymer matrix owing to favorable Ag flake-Ag flake interactions (Fig. 3c).³⁸ The results showed that the rearrangement of the Ag flakes occurred even in the conductive composite thin film soaked between fiber bundles. A similar trend was observed in the sample subjected to the heat and pressure treatments.

3.3 Cyclic endurance of the conductive fabrics

To characterize the endurance of the developed conductive fabric, we performed a cyclic test at a strain of 25% (Fig. 3d). The relative change in resistance for the pristine conductive fabric after 1000 cycles at a strain of 25% shows drastic or unstable resistance change during the cyclic stretching ($\Delta R/R_0 \sim 70$). The modulus mismatch between the conductive composite and the fabric induces the stress to the soaked composite film, resulting in an abrupt change in resistance. By contrast, the resistance of the MED-ET increased by less than a factor of 0.25 by effective stress relaxation of the kirigami pattern. Furthermore, the sample subjected to heat and pressure treatments exhibited a slight improvement in the resistance change during the cyclic test (Fig. 3e). Also, the sample showed a stable electrical performance ($\Delta R/R_0 \sim 0.8$) under the cyclic test at 50% strain (Fig. S5†). This result could be explained by the amount of ink delivered to the textile when heat and pressure were applied.⁴⁰

3.4 Demonstration of stretchable LED interconnected with the MED-ET

As a proof-of-concept example of the electrical recovery in the developed conductive fabric, we prepared a micro-LED interconnected with the MED-ET, as shown in Fig. 4a. After turning the LED on by applying a voltage, we scratched the conductive fabric using a blade four times in the same region, and the

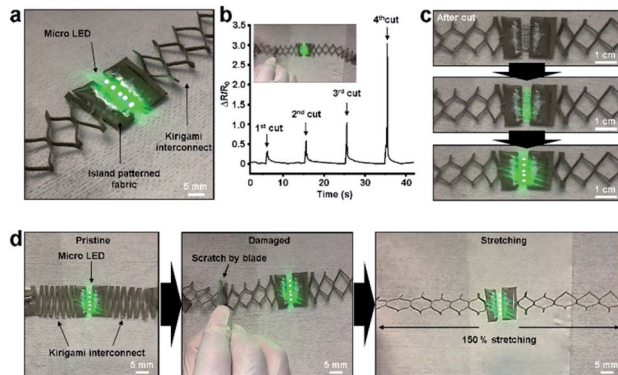


Fig. 4 Electrical recoverability of MED-ET for robust micro-LED interconnections. (a) Photograph of a micro-LED interconnected with MED-ET. (b) Relative changes in the resistance of the interconnections during the fourth scratching process. The electrical performance of the interconnection was well recovered after scratching. The inset shows a photograph of the scratching process. (c) Restored brightness of the micro-LED over time after the fourth scratching process. (d) Photograph of the sequential process for pristine, scratching, and stretching.

applied force was increased each time (Fig. 4b). During the fourth scratching process, an abrupt change in resistance occurred, followed by the recovery of resistance to the initial value. As expected, the rearrangement of Ag flakes in the damaged area occurred even at the $\sim 20 \mu\text{m}$ scale of the composite film soaked between fiber bundles during the test involving four scratches.^{38,42,43} This electrical recovery was clearly indicated by the change and the maintenance in the brightness of the micro-LED. The micro-LED turned off instantaneously after the fourth cut, but the brightness of the micro-LED was restored within 3 s (Fig. 4c and Video S1†). As an extreme case, we observed the successful operation of the micro-LED after a sequential process involving repetitive scratching and stretching (Fig. 4d).

3.5 Demonstration of EMG measurements

To demonstrate the ability of the developed conductive fabric to detect physiological signals, we applied the MED-ET to an EMG monitoring system (Fig. S6†). We prepared three MED-ET interconnections, which were assigned as the reference, active (+), and ground (−), as shown in Fig. 5a. This system was conformally attached to the skin by covering it with a transparent

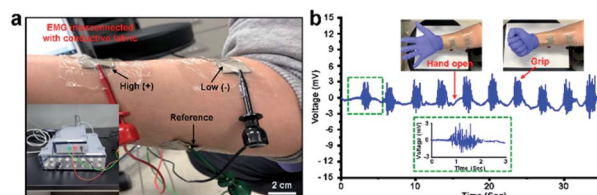


Fig. 5 Real-time electromyogram (EMG) monitoring using the developed MED-ET. (a) Photo image of measurement set up of EMG monitoring. (b) Detection of EMG signal from our MED-ETs in real-time.



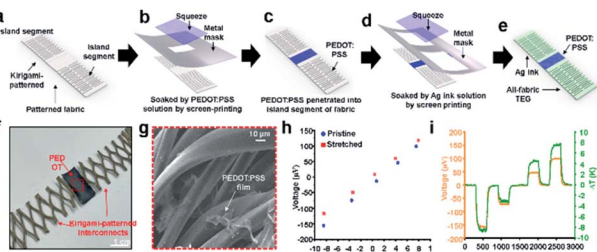


Fig. 6 All-fabric thermoelectric generator (F-TEG) interconnected with-ET. (a) First, kirigami-patterned fabric with island segments was prepared. (b), (c) Subsequently, the fabric with island segments was soaked in PEDOT:PSS solution via the screen-printing method. In the same manner, (d), (e) the kirigami-patterned fabric was soaked in Ag ink for fabricating interconnections (f) photograph of the F-TEG comprising the PEDOT:PSS island and interconnections of MED-ET. (g) Cross-sectional SEM image of the textile soaked in PEDOT:PSS solution. (h) Relationship between voltage generation in the F-TEG (V_{thermal}) and temperature differences (ΔT). (i) Voltage generation in the F-TEG placed on a hot object.

skin patch (3M Tegaderm, USA). The interconnects formed using the MED-ET enabled real-time EMG monitoring for muscle contractions of the forearm flexor, without requiring the conventional conductive wet gels (Fig. 5b).⁴⁴ For a long-term reliable EMG monitoring system, the Ag flakes can be coated by biocompatible inert metal to minimize the effects of biofluidic environment.^{45,46}

3.6 Demonstration of stretchable thermoelectric generator

We fabricated an all-fabric thermal electric generator (F-TEG) consisting of poly(3,4-ethylenedioxothiophene) polystyrene sulfonate (PEDOT:PSS) and a MED-ET interconnection. To fabricate this device (Fig. 6a–e), we first soaked the island segment of the fabric in the PEDOT:PSS solution; this was followed by annealing at 100 °C in an oven.^{47,48} Fig. 6f shows a photograph of the overall device structure. A scanning electron microscopy (SEM) image of the fabric soaked in PEDOT:PSS is shown in Fig. 6g. The water-based PEDOT:PSS solution penetrated well into the fabric owing to the hydrophilic surface of the polyurethane-based fabric. After forming the PEDOT layer, tough self-healing stretchable ink penetrated the kirigami-shaped segments of fabric on both sides of the island. To characterize the as-fabricated F-TEG, we induced a temperature difference to observe the generated voltage. Fig. 6h, the relationship between the voltage generation in the F-TEG and the temperature differences. Based on the graph, the Seebeck coefficient was calculated to be 15.8 $\mu\text{V K}^{-1}$. To evaluate the effects of stretching on the thermoelectric performance, we measured the thermovoltage of the F-TEG films under the 100% stretching condition (14.5 $\mu\text{V K}^{-1}$ at a strain of 100% for the kirigami-shaped interconnection), as shown in Fig. 6h. Owing to these kirigami interconnections, the F-TEG thermovoltage was well-preserved at a strain of 100%. Lastly, we evaluated the reliability of the F-TEG at different temperatures over time, as shown in Fig. 6i.

4 Conclusions

In this study, we designed a MED-ET to realize high stretchability and a low modulus; these properties were achieved using kirigami patterns, which afforded strain relaxation. Furthermore, we observed that electrical recovery occurred in the tough self-healing stretchable inks coated uniformly on the three-dimensional surface of the fabric. The results show that the Ag flakes in the polymer are rearranged even in thin films coated over various surfaces. To improve mechanical and electrical stability, we applied heat and pressure to the MED-ET. Furthermore, through the demonstration of a micro-LED, we highlighted the electrical recovery of the developed MED-ET. To determine the feasibility of applying this conductive fabric in wearable electronics, real-time EMG monitoring was performed; physiological signals were successfully detected using the conductive fabrics. Finally, an F-TEG was demonstrated to suggest potential textile-based, energy-harvesting devices.

Conflicts of interest

There are no conflicts to declare.

Acknowledgements

This work was supported by the National Research Foundation of Korea (NRF) grant funded by the Korean government (MSIT) (No 2020R1C1C1005567). This work was also supported by the Creative-Pioneering Researchers Program through Seoul National University. This research was partially supported by Institute for Basic Science (IBS-R015-D1)

Notes and references

- Z. Zhang, L. Cui, X. Shi, X. Tian, D. Wang, C. Gu, E. Chen, X. Cheng, Y. Xu, Y. Hu, J. Zhang, L. Zhou, H. H. Fing, P. Ma, G. Jiang, X. Sun, B. Zhang and H. Peng, Textile Display for Electronic and Brain-Interfaced Communications, *Adv. Mater.*, 2018, **30**, 1800323.
- Y. H. Hwang, S. Kwon, J. B. Shin, H. Kim, Y. H. Son, H. S. Lee, B. Noh, M. Nam and K. C. Choi Bright-Multicolor, Highly Efficient, and Addressable Phosphorescent Organic Light-Emitting Fibers: Toward Wearable Textile Information Displays, *Adv. Funct. Mater.*, 2021, **31**, 2009336.
- S. Kwon, W. Kim, H. Kim, S. Choi, B. C. Park, S. H. Kang and K. C. Choi, High Luminance Fiber-Based Polymer Light-Emitting Devices by a Dip-Coating Method, *Adv. Electron. Mater.*, 2015, **1**, 1500103.
- A. Komolafe, R. Torah, Y. Wei, H. Nunes-Matos, M. Li, D. Hardy, T. Dias, M. Tudor and S. Beeby, Integrating Flexible Filament Circuits for E-Textile Applications, *Adv. Mater. Technol.*, 2019, **4**, 1900176.
- J. Chen, Y. Huang, N. Zhang, H. Zou, R. Liu, C. Tao, X. Fan and W. Z. Lin, Micro-cable structured textile for simultaneously harvesting solar and mechanical energy, *Nat. Energy*, 2016, **1**, 16138.



6 Z. Chai, N. Zhang, P. Sun, Y. Huang, C. Zhao, H. J. Fan, X. Fan and W. Mai, Tailorable and Wearable Textile Devices for Solar Energy Harvesting and Simultaneous Storage, *ACS Nano*, 2016, **10**, 9201–9207.

7 J. Xiong, P. Cui, X. Chen, J. Wang, K. Parida, M. F. Lin and P. S. Lee, Skin-touch-actuated textile-based triboelectric nanogenerator with black phosphorus for durable biomechanical energy harvesting, *Nat. Commun.*, 2018, **9**, 4280.

8 J. Lee, H. Kwon, J. Seo, S. Shin, J. H. Koo, C. Pang, S. Son, J. H. Kim, Y. H. Jang, D. E. Kim and T. Lee, Conductive Fiber-Based Ultrasensitive Textile Pressure Sensor for Wearable Electronics, *Adv. Mater.*, 2015, **27**, 2433–2439.

9 Z. Wen, M. H. Yeh, H. Guo, J. Wang, Y. Zi, W. Xu, J. Deng, L. Zhu, X. Wang, C. Hu, L. Zhu, X. Sun and Z. L. Wang, Self-powered textile for wearable electronics by hybridizing fiber-shaped nanogenerators, solar cells, and supercapacitors, *Sci. Adv.*, 2016, **2**, e1600097.

10 Z. Zhao, C. Yan, Z. Liu, X. Fu, L. M. Peng, Y. Hu and Z. Zheng, Machine-Washable Textile Triboelectric Nanogenerators for Effective Human Respiratory Monitoring through Loom Weaving of Metallic Yarns, *Adv. Mater.*, 2016, **28**, 10267–10274.

11 W. Fan, Q. He, K. Meng, X. Tan, Z. Zhou, G. Zhang, J. Yang and Z. L. Wang, Machine-knitted washable sensor array textile for precise epidermal physiological signal monitoring, *Sci. Adv.*, 2020, **6**, eaay2840.

12 X. Shi, Y. Zuo, P. Zhai, J. Shen, Y. Yang, Z. Gao, M. Liao, J. Wu, J. Wang, X. Xu, Q. Tong, B. Zhang, B. Wang, X. Sun, L. Zhang, Q. Pei, D. Jin, P. Chen and H. Peng, Large-area display textiles integrated with functional systems, *Nature*, 2021, **591**, 240.

13 M. J. Yun, Y. H. Sim, D. Y. Lee and S. I. Cha, Highly stretchable large area woven, knitted and robust braided textile based interconnection for stretchable electronics, *Sci. Rep.*, 2021, **11**, 4038.

14 H. Kim, T. H. Kang, J. Ahn, H. Han, S. Park, S. J. Kim, M. C. Park, S. H. Paik, D. K. Hwang, H. Yi and J. A. Lim, Spirally Wrapped Carbon Nanotube Microelectrodes for Fiber Optoelectronic Devices beyond Geometrical Limitations toward Smart Wearable E-Textile Applications, *ACS Nano*, 2020, **14**, 17213–17223.

15 J. S. Heo, K. W. Lee, J. H. Lee, S. B. Shin, J. W. Jo, Y. H. Kim, M. G. Kim and S. K. Park, Highly-Sensitive Textile Pressure Sensors Enabled by Suspended-Type All Carbon Nanotube Fiber Transistor Architecture, *Micromachines*, 2020, **11**, 1103.

16 I. D. Agua, D. Mantione, U. Ismailov, A. Sanchez-Sanchez, N. Aramburu, G. G. Malliaras, D. Mecerreyres and E. Ismailova, DVS-Crosslinked PEDOT:PSS Free-Standing and Textile Electrodes toward Wearable Health Monitoring, *Adv. Mater. Technol.*, 2018, **3**, 1700322.

17 H. M. Elmoughni, A. K. Menon, R. M. W. Wolfe and S. K. Yee, A Textile-Integrated Polymer Thermoelectric Generator for Body Heat Harvesting, *Adv. Mater. Technol.*, 2019, **4**, 1800708.

18 P. Zhu, J. Zhu, C. Yan, M. Dirican, J. Zang, H. Jia, Y. Li, Y. Kiyak, H. Tan and X. Zhang, In Situ Polymerization of Nanostructured Conductive Polymer on 3D Sulfur/Carbon Nanofiber Composite Network as Cathode for High-Performance Lithium-Sulfur Batteries, *Adv. Mater. Interfaces*, 2018, **5**, 1701598.

19 L. C. Jia, K. Q. Ding, R. J. Ma, H. L. Wang, W. J. Sun, D. X. Yan, B. Li and Z. M. Li, Highly Conductive and Machine-Washable Textiles for Efficient Electromagnetic Interference Shielding, *Adv. Mater. Technol.*, 2019, **4**, 1800503.

20 L.-X. Liu, W. Chen, H. B. Zhang, Q. W. Wang, F. Guan and Z. Z. Yu, Flexible and Multifunctional Silk Textiles with Biomimetic Leaf-Like MXene/Silver Nanowire Nanostructures for Electromagnetic Interference Shielding, Humidity Monitoring, and Self-Derived Hydrophobicity, *Adv. Funct. Mater.*, 2019, **29**, 1905197.

21 L. Cai, A. Y. Song, P. Wu, P. C. Hsu, Y. Peng, J. Chen, C. Liu, P. B. Catrysse, Y. Liu, A. Yang, C. Zhou, C. Zhou, S. Fan and Y. Cui, Warming up human body by nanoporous metallized polyethylene textile, *Nat. Commun.*, 2017, **8**, 496.

22 X. Pu, L. Li, M. Liu, C. Jiang, C. Du, Z. Zhao, W. Hu and Z. L. Wang, Wearable Self-Charging Power Textile Based on Flexible Yarn Supercapacitors and Fabric Nanogenerators, *Adv. Mater.*, 2015, **28**, 98–105.

23 S. H. Kim, S. Jung, I. S. Yoon, C. Lee, Y. Oh and J.-M. Hong, Ultrastretchable Conductor Fabricated on Skin-Like Hydrogel-Elastomer Hybrid Substrates for Skin Electronics, *Adv. Mater.*, 2018, **30**, 1800109.

24 N. Matsuhisa, M. Kaltenbrunner, T. Yokota, H. Jinno, K. Kuribara, T. Sekitani and T. Someya, Printable elastic conductors with a high conductivity for electronic textile applications, *Nat. Commun.*, 2015, **6**, 7461.

25 D. Li, W. Y. Lai, Y. Z. Zhang and W. Huang, Printable Transparent Conductive Films for Flexible Electronics, *Adv. Mater.*, 2018, **30**, 1704738.

26 T. Sekitani, Y. Noguchi, K. Hata, T. Fukushima, T. Aida and T. Someya, A Rubberlike Stretchable Active Matrix Using Elastic Conductors, *Science*, 2008, **321**, 1468–1472.

27 A. Russo, B. Y. Ahn, J. J. Adams, E. B. Duoss, J. T. Bernhard and J. A. Lewis, Pen-on-Paper Flexible Electronics, *Adv. Mater.*, 2011, **23**, 3426–3430.

28 S. Niu, N. Matsuhisa, L. Beker, J. Li, S. Wang, J. Wang, Y. Jiang, X. Yan, Y. Yun, W. Burnett, A. S. Y. Poon, J. B.-H. Tok, X. Chen and Z. Bao, A wireless body area sensor network based on stretchable passive tags, *Nat. Electron.*, 2019, **2**, 361–368.

29 P. Won, J. J. Park, T. Lee, I. Ha, S. Han, M. Choi, J. Lee, S. Hong, K. J. Cho and S. H. Ko, Stretchable and Transparent Kirigami Conductor of Nanowire Percolation Network for Electronic Skin Applications, *Nano Lett.*, 2019, **19**, 6087–6096.

30 Y. S. Guan, Z. Zhang, Y. Tang, J. Yin and S. Ren, Kirigami-Inspired Nanoconfined Polymer Conducting Nanosheets with 2000% Stretchability, *Adv. Mater.*, 2018, **30**, 1706390.

31 Z. Zhang, Y. Yu, Y. Tang, Y. S. Guan, Y. Hu, J. Yin, K. Willets and S. Ren, Kirigami-Inspired Stretchable Conjugated Electronics, *Adv. Electron. Mater.*, 2020, **6**, 1900929.



32 T. C. Shyu, P. F. Damasceno, P. M. Dodd, A. Lamoureux, L. Xu, M. Shlian, M. Shtein, S. C. Glotzer and N. A. Kotov, A kirigami approach to engineering elasticity in nanocomposites through patterned defects, *Nat. Mater.*, 2015, **14**, 785–789.

33 Y. S. Guan, H. Li, F. Ren and S. Ren, Kirigami-Inspired Conducting Polymer Thermoelectrics from Electrostatic Recognition Driven Assembly, *ACS Nano*, 2018, **12**, 7967–7973.

34 Y. Morikawa, S. Yamagiwa, H. Sawahata, R. Numan, K. Koida, M. Ishida and T. Kawano, Ultrastretchable Kirigami Bioprosbes, *Adv. Healthcare Mater.*, 2018, **7**, 1701100.

35 M. K. Blees, A. W. Barnard, P. A. Rose, S. P. Roberts, K. L. McGill, P. Y. Huang, A. R. Ruyack, J. W. Kevek, B. Kobrin, D. A. Muller and P. L. McEuen, Graphene kirigami, *Nature*, 2015, **524**, 204.

36 A. Rafsanjani, Y. Zhang, B. Liu, S. M. Rubinstein and K. Bertoldi, Kirigami skins make a simple soft actuator crawl, *Sci. Robot.*, 2018, **3**, eaar7555.

37 B. M. Li, I. Kim, Y. Zhou, A. C. Mills, T. J. Flewelling and J. S. Jur, Kirigami-Inspired Textile Electronics: K.I.T.E., *Adv. Mater.*, 2019, **4**, 1900511.

38 S. H. Kim, H. Seo, J. Kang, J. Hong, D. Seong, H. J. Kim, J. Kim, J. Mun, I. Youn, J. Kim, Y. C. Kim, H. K. Seok, C. Lee, J. B.-H. Tok, Z. Bao and D. Son, An Ultrastretchable and Self-Healable Nanocomposite Conductor Enabled by Autonomously Percolative Electrical Pathways, *ACS Nano*, 2019, **13**, 6531–6539.

39 J. Kang, D. Son, G. J. N. Wang, Y. Liu, J. Lopez, Y. Kim, J. Y. Oh, T. Katsumata, J. Mun, Y. Lee, L. Jin, J. B.-H. Tok and Z. Bao, Tough and Water Insensitive Self-Healing Elastomer for Robust Electronic Skin, *Adv. Mater.*, 2018, **30**, 1706846.

40 H. Jin, N. Matsuhisa, S. Lee, M. Abbas, T. Yokota and T. Someya, Enhancing the Performance of Stretchable Conductors for E-Textiles by Controlled Ink Permeation, *Adv. Mater.*, 2017, **29**, 1605848.

41 C. S. Boland, U. Khan, G. Ryan, S. Barwick, R. Charifou, A. Harvey, C. Backes, Z. Li, M. S. Ferreira, M. E. Möbius, R. J. Young and J. N. Coleman, Sensitive electromechanical sensors using viscoelastic graphene-polymer nanocomposites, *Science*, 2016, **354**, 1257.

42 D. Son, J. Kang, O. Vardoulis, Y. Kim, N. Matsuhisa, J. Y. Oh, J. W. F. To, J. Mun, T. Katsumata, Y. Liu, A. F. McGuire, M. Krason, F. Molina-Lopez, J. Ham, U. Kraft, Y. Lee, Y. Yun, J. B.-H. Tok and Z. Bao, An integrated self-healable electronic skin system fabricated via dynamic reconstruction of a nanostructured conducting network, *Nat. Nanotechnol.*, 2018, **13**, 1057–1065.

43 B. C.-K. Tee, C. Wang, R. Allen and Z. Bao, An electrically and mechanically self-healing composite with pressure- and flexion-sensitive properties for electronic skin applications, *Nat. Nanotechnol.*, 2012, **7**, 825–832.

44 D. Roman-Liu and P. Bartuzi, The influence of wrist posture on the time and frequency EMG signal measures of forearm muscles, *Gait Posture*, 2013, **37**, 340–344.

45 S. Choi, S. I. Han, D. Jung, H. J. Hwang, C. Lim, S. Bae, O. K. Park, C. M. Tschabrunn, M. Lee, S. Y. Bae, J. W. Yu, J. H. Ryu, S.-W. Lee, K. Park, P. Kang, W. B. Lee, R. Nezafat, T. Hyeon and D.-H. Kim, Highly conductive, stretchable and biocompatible Ag–Au core–sheath nanowire composite for wearable and implantable bioelectronics, *Nat. Nanotechnol.*, 2018, **13**, 1048–1056.

46 H. Seo, S. I. Han, K.-I. Song, D. Seong, K. Lee, S. H. Kim, T. Park, J. H. Koo, M. Shin, H. W. Baac, O. K. Park, S. J. Oh, H.-S. Han, H. Jeon, Y.-C. Kim, D.-H. Kim, T. Hyeon and D. Son, Durable and Fatigue-Resistant Soft Peripheral Neuroprosthetics for In Vivo Bidirectional Signaling, *Adv. Mater.*, 2021, **33**, 2007346.

47 Y. Lee, J. Park, J. Son, H. Y. Woo and J. Kwak, Degenerately Doped Semi-Crystalline Polymers for High Performance Thermoelectrics, *Adv. Funct. Mater.*, 2021, **31**, 2006900.

48 Z. Fan and J. Ouyang, Thermoelectric Properties of PEDOT:PSS, *Adv. Electron. Mater.*, 2019, **5**, 1800769.

